Atmos. Meas. Tech. Discuss., 8, 10523–10548, 2015
www.atmos-meas-tech-discuss.net/8/10523/2015/
doi:10.5194/amtd-8-10523-2015

Atmospheric Measurement Techniques Discussions
Open Access

Retrieval of xCO_2 from ground-based mid-infrared (NDACC) solar absorption spectra and comparison to TCCON

M. Buschmann[1], N. M. Deutscher[1,2], V. Sherlock[3], M. Palm[1], T. Warneke[1], and J. Notholt[1]

[1]Institute of Environmental Physics, University of Bremen, Bremen, Germany
[2]School of Chemistry, University of Wollongong, Wollongong, NSW, Australia
[3]Department of Atmospheric Research, National Institute of Water and Atmospheric Research (NIWA) Ltd, Wellington, New Zealand

Received: 3 August 2015 – Accepted: 25 September 2015 – Published: 14 October 2015

Correspondence to: M. Buschmann (m_buschmann@iup.physik.uni-bremen.de)

Published by Copernicus Publications on behalf of the European Geosciences Union.

Abstract

High resolution solar absorption spectra, taken within the Network for the Detection of Atmospheric Composition Change (NDACC) in the mid-infrared spectral region are used to infer partial or total column abundances of many gases. In this paper we present the retrieval of a column averaged mole fraction of carbon dioxide from NDACC-IRWG spectra taken with a Fourier-Transform-Infra-Red (FTIR) spectrometer at the site in Ny-Ålesund, Spitsbergen. The retrieved time series is compared to co-located standard TCCON measurements of total column CO_2. Comparing the NDACC and TCCON retrievals we find that the sensitivity of the NDACC retrieval is lower in the troposphere (by a factor of two) and higher in the stratosphere, compared to TCCON. Thus, the NDACC retrieval is less sensitive to tropospheric changes (e.g. the seasonal cycle) in the column average.

1 Introduction

The continued measurement of atmospheric trace gases, especially in the context of climate change, has given valuable insight on their sources and sinks (Ciais et al., 2013). In-situ measurements offer high accuracy and repeatability, but are spatially highly constrained and influenced by local perturbations. Remote sensing instruments are less influenced by boundary layer processes and can provide complementary information to in-situ measurements because they sample the total atmospheric column.

A world wide network of Fourier Transform InfraRed (FTIR) spectrometers acquires solar absorption spectra from which total columns of a number of gases are retrieved. The Network for the Detection of Atmospheric Composition Change (NDACC) provides timeseries of mid-infrared (MIR) solar absorption spectra at various sites dating back to 1978 (Kitt Peak Observatory). Since its inception in 2004, the Total Carbon Column Observing Network (TCCON) has created a high quality database of near infrared (NIR) solar absorption spectra. Both networks have been used to deduce total column

AMTD
8, 10523–10548, 2015

amounts of various atmospheric constituents, the main focus being centered around O_3-Chemistry (NDACC, see e.g. Notholt et al., 1995) and the carbon cycle (TCCON, see e.g. Wunch et al., 2011a).

TCCON retrievals of the dry-air mole fraction of CO_2 employ a method of ratioing CO_2 from the 6300 cm^{-1} band to O_2, measured simultaneously from the 7885 cm^{-1} band (Yang et al., 2002). This approach compensates for common systematic errors (like light path variations and pointing errors). Additionally the selected spectral windows in the NIR have few interfering gases, allowing for high quality spectral fits. This results in a network wide accuracy of the TCCON data of around 0.2 % for xCO_2.

However, near-infrared (TCCON) measurements are only available since 2004 (with many sites starting operation more recently). An extension of the retrieval capabilities to the mid-infrared (NDACC) spectra would expand the total column products not only in time, but would also expand the spatial coverage. Two major challenges have to be faced on the way to a NDACC xCO_2 product: in contrast to the NIR, there are no O_2 absorption lines present in the MIR spectra, therefore there is no proxy for the dry air column to which to ratio. Additionally the presence of multiple interfering gases hinders the use of broad spectral windows.

This study was undertaken within the framework of ESA's Greenhouse Gas Climate Change Initiative (Buchwitz et al., 2013). Its aim is to assess whether MIR FTIR spectra could be used to derive a total column CO_2 mole fraction. A similar analysis has already been performed for the MIR retrieval of CH_4 in Sussmann et al. (2013). Recently, Barthlott et al. (2015) used MIR xCO_2 retrievals in combination with a simple model to investigate the long term consistency of NDACC measurements.

In this paper we describe the retrieval of the column average dry-air mole fraction of CO_2 (denoted xCO_2) in the MIR, discuss the differing retrieval sensitivities from the NIR and the dependency of the retrieval on the a priori information. We conclude that it is possible to retrieve xCO_2 from NDACC spectra. The secular increase of xCO_2 is well captured. Information on the seasonal cycle, however, is mainly introduced by the

AMTD
8, 10523–10548, 2015

a priori. We show that this is caused by the different averaging kernels, which show that the NDACC xCO_2 retrievals are most sensitive to the stratospheric CO_2.

In the second section we describe the microwindows used in the retrieval and then continue with a description of the retrieval methods for the MIR and briefly for the NIR. In the third and fourth sections we investigate the influence of both the a priori and averaging kernels on the retrieval in comparison to TCCON. We conclude with a summary of the results.

2 Methods

2.1 Measurement site

For this study we chose the station in Ny-Ålesund (78.92° N, 11.92° E) for its long time series and the large seasonal cycle of xCO_2. The instrument used is a Bruker IFS 120HR Fourier-Transform-InfraRed spectrometer. MIR spectra have been taken since 1992, while since 2004 NIR spectra within TCCON have also been measured. Measurements are taken under cloud-free conditions alternately in the MIR and NIR. Due to its high latitude, no solar absorption measurements can be taken in Ny-Ålesund during the polar night.

2.2 CO_2 microwindows in the mid-infrared

In the mid-infrared region (between 2000 and 4000 cm^{-1}) in addition to CO_2, other (interfering) gases have strong absorption lines. Some spectral regions are dominated by the interference gases, while in others CO_2 is the most prominent feature. This makes it impractical to select whole absorption bands for the retrieval, such as is done in the NIR by the TCCON. The high resolution NDACC spectra allow the selection of microwindows that contain only single lines. The contribution of interfering gases to the single line shapes varies for different microwindow.

AMTD
8, 10523–10548, 2015

Multiple microwindows are fitted in three spectral regions: four microwindows at around 2624 cm^{-1}, two microwindows at 3160 cm^{-1} and two around 3330 cm^{-1}. The corresponding line parameters are taken from the GGG linelist, which is based on the HITRAN database Rothman et al. (2005, 2009). These are shown in Table 1. Each of the spectral regions referred to above corresponds to a different optical filter or detector setting, and they are measured sequentially at acquisition. The retrieval is performed separately for each spectral interval and microwindow. Following this approach we obtain eight different retrievals of xCO_2 (one for each microwindow).

Retrievals from microwindows within the same spectral interval were averaged, and used to derive daily averages to correlate with the daily-averaged TCCON retrievals. This approach circumvents the temporal coincidence problem that arises due to the different acquisition procedures described in Sect. 2.1.

2.3 xCO_2 retrieval

The MIR xCO_2 retrieval has been performed with the profile scaling algorithm GFIT (version 4.8.6 in GGG2012), which is also used for the TCCON xCO_2 retrievals. In GFIT a priori profiles of the target gas, gases of interest, and pressure, temperature and H_2O are convolved with an instrument lineshape model to simulate a spectrum. The gas profiles are scaled and other spectral parameters adjusted to provide the best fit to the measured spectrum by minimizing the residual. From these scaled profiles, the amount of the target gas is retrieved. An example fit is shown in Fig. 1.

The standard TCCON retrieval uses O_2, retrieved from the same spectra as the target gases in the band at 7885 cm^{-1}, to estimate the total dry-air column. The retrieved CO_2 column is then ratioed to this retrieved O_2 column to derive the column average dry-air mole fraction. The method is explained in further detail in Wunch et al. (2011a).

The same software version was used to analyze the MIR spectra. To benefit from the above mentioned ratioing approach, a MIR active species with a well-known atmospheric abundance would be needed. Only N_2 has some weak absorption lines in the target region: its multipolar $1 \rightarrow 0$ transition. The suitability of these lines for atmo-

AMTD
8, 10523–10548, 2015

spheric retrieval was previously investigated by Goldman et al. (2007). Due to the very low intensity, the retrieved N_2 mole fractions introduced more noise than was compensated by the ratioing, meaning that N_2 was not able to be used as an internal standard.

Instead, mole fractions from the MIR spectra are calculated by normalization by the dry air column abundance inferred from an independent measurement of surface pressure. The vertical column of H_2O was also retrieved from a dedicated H_2O microwindow in the vicinity of the respective CO_2 microwindow. Total column CO_2 was then calculated as described in Appendix A in Wunch et al. (2011b) by applying:

$$xCO_2 = \frac{VC_{CO_2}}{\frac{P_s}{\langle g_{air}\rangle - m_{air}^{dry}} - \frac{VC_{H_2O}\cdot m_{H_2O}}{m_{air}}} \quad (1)$$

Here, m_{air} and m_{H_2O} denote the molecular masses of dry-air and water, respectively, P_s the surface pressure, and $\langle g_{air}\rangle$ the column averaged gravitational acceleration. VC_{CO_2} and VC_{H_2O} are the retrieved vertical column amounts from the GFIT output.

The retrieved dry-air mole fractions are then quality controlled by removing data points with high solar zenith angles ($> 80^\circ$) and/or with a high relative retrieval error ($> 20\,\%$). Table 2 shows uncertainty estimates for the resulting time series, based on the standard deviation of the daily means. The mean of the standard deviations for the three microwindow regions is compared to the standard TCCON results. Additionally the standard error is shown in order to better reflect the certainty in the daily mean, which is also influenced by the number of measurements within each day. Only days with two or more measurements have been used. This approach results in an error estimate (1σ) of 1.13 ppm for the Ny-Ålesund TCCON standard product ($\approx 0.3\,\%$) and 2.06 ppm (0.5 %) for the 2600 cm^{-1} microwindow, respectively (see Table 2).

AMTD
8, 10523–10548, 2015

3 Influence of a priori information

Following Rodgers (2000) and Rodgers and Connor (2003) the retrieval of the total column abundance ($\hat{x}$) as described above depends (for a true quantity x) on both the choice of the a priori profile (x_a) and the measurements averaging kernel (A). Thus, Eq. (3) in Rodgers and Connor (2003) gives:

$$\hat{x} - x_a = A(x - x_a) + \epsilon_x \quad (2)$$

where ϵ_x is the (random and systematic) error term. If the measurement information content does not fully constrain the retrieval, the result will be influenced by the a priori. Within TCCON a (latitude and time dependent) empirical model is used to simulate an xCO_2 profile that is already quite close to the true atmospheric profile. There is one TCCON a priori profile per day calculated for local noon. These are shown in Fig. 2.

Usage of this modeled a priori profile in the MIR retrieval can give an overly-favorable impression of the information content of the MIR retrieval, i.e. even if there is no additional information to be retrieved from the spectra, still a reasonably good agreement between the NIR and MIR retrievals is to be expected because the smoothing error term tends to zero when the prior is approximately equal to the true atmospheric state (for a detailed explanation see Sect. 4).

To investigate this, xCO_2 has been retrieved from both MIR and NIR spectra, once using the standard (time dependent) TCCON a priori, and once using a fixed, constant a priori profile of 379 ppm throughout the atmosphere. Apart from the different a priori, the same retrieval and post processing parameters have been used as in the original retrievals (with the TCCON a priori).

The comparison of the NIR (TCCON) time series with modeled and fixed a prioris shows a clear pattern. This corresponds to an overestimation of the seasonal cycle amplitude by the retrieval using a fixed a priori compared to the standard a priori. At seasonal maximum the difference is negative and at the seasonal minimum positive, respectively. The same pattern can be deduced from the slope in the correlation plot

AMTD
8, 10523–10548, 2015

in Fig. 3. This can be attributed to the usage of a fixed a priori in conjunction with the solar zenith angle dependent averaging kernel (see Fig. 4). The solar zenith angles are generally larger in spring and autumn than in summer. The TCCON averaging kernels show an increased sensitivity in the troposphere. This coincides with the seasonal maximum of xCO_2 in spring and with the seasonal minimum in autumn. In these cases the TCCON averaging kernel diverges from being close to a unit vector and subsequently the smoothing error contributions increase if the prior differs from the true atmospheric state. Thus the residual pattern in Fig. 3 originates from the shape of the averaging kernels.

In the case of the MIR NDACC spectra, the results of the retrieval with the TCCON a priori in comparison to that with a fixed a priori can be seen in Fig. 5. Both time series (the NDACC retrieval with the TCCON a priori and that with the fixed a priori) capture the secular trend and no residual trend is visible. The seasonal cycle amplitude, however, is damped in the NDACC retrieval (shown here are the results of the 2600 cm^{-1} microwindow, other regions show comparable results). A clear seasonal structure can be seen in the residual.

In order to quantify the effect the different a priori information has on the retrievals, a simple function (see Eq. 3) has been fitted to each time series (see Fig. 6):

$$xCO_2(t) = a + b \cdot t + A \cdot \sin(2\pi \cdot t) \quad (3)$$

where a is an offset at the beginning of the partial time series (1 January 2009), b is the linear trend per year and A the amplitude of the seasonal cycle. The fit parameters are presented in Table 3. The comparison of the fitted amplitudes of the time series of the different retrievals allows for an estimate of the magnitude of the damping of the seasonal cycle amplitude.

The results show a slight increase from the case of the standard TCCON retrieval to the TCCON retrieval with a fixed a priori by a factor of 1.14 (as was discussed earlier and can be seen in the correlation plot in Fig. 3). However, the fixed a priori NDACC retrieval shows a decrease in the seasonal cycle amplitude. The amplitude of

AMTD
8, 10523–10548, 2015

the NDACC retrieval with modeled a priori is found to be 2.12 times larger than the amplitude of the fixed a priori NDACC retrieval.

Similar to the approach used above for the TCCON case, we now investigate whether this is due to the differences in the averaging kernel, i.e. the sensitivity of the retrievals to different height levels. The tropospheric (or stratospheric) contribution of a retrieval can be estimated by integrating the averaging kernels for a retrieval (normalized on a pressure grid) over the contributing pressure column. Thus, the averaging kernels have been integrated in two parts, separated at the tropopause height at 300 hPa (see Fig. 7).

As can be seen in Fig. 4, in contrast to the NDACC xCO_2 kernels the TCCON averaging kernels strongly vary with the solar zenith angle. This leads to a zenith angle dependent ratio between the stratospheric and tropospheric contribution of the averaging kernels.

For the presented time series of NDACC xCO_2 from the 2600 cm^{-1} microwindow the average solar zenith angle is 69°. For this angle, a ratio of 2.05 between the tropospheric averaging kernel contribution of TCCON to NDACC xCO_2 can be calculated. Values of 1.80 and 2.18 are calculated for solar zenith angles of 40 and 80°, respectively. Assuming that variability in CO_2 occurs solely in the troposphere (i.e. that the seasonal variation in the stratosphere is negligible), a change in tropospheric CO_2 would result in a signal that is retrieved as being two times smaller than that retrieved from TCCON. This is in good agreement with the tropospheric contribution calculated from the time series' fits with a fixed a priori described above (2.12).

4 Averaging kernel smoothing error estimation

After investigating the influence of a varying a priori profile on the retrieval results presented above, in the following the effect the different shape of the averaging kernels (given a common a priori) has on the retrieved xCO_2 is addressed. The differently

AMTD
8, 10523–10548, 2015

shaped averaging kernels (see Fig. 4) must be taken into account in a direct comparison of the NDACC and TCCON xCO_2 products (Rodgers and Connor, 2003).

The general difference in the averaging kernel shape originates from the (compared to the NIR) narrow absorption lines in the MIR. Thus the NDACC xCO_2 averaging kernels show a higher sensitivity at lower atmospheric pressures.

We can quantify the differences between the two retrievals we expect to find for a given, true atmospheric state using a common prior. This is then an estimate of the averaging kernel smoothing error. Following the derivation in Sect. 4.3 in Rodgers and Connor (2003) and in Appendix A of Wunch et al. (2011b), two total column retrievals of a remote sounding instrument can be compared by choosing a common a priori x_c and a *true* atmospheric CO_2 profile x. The difference of two retrieved total column amounts contributed by the different averaging kernels, is then:

$$c_{\text{corr}} = \frac{1}{p_0} \sum_j \Delta p_j \left(a_j^{\text{mir}} - a_j^{\text{nir}} \right) (x - x_a) \tag{4}$$

with the surface pressure p_0, the column averaging kernels a, *true* profile x and the common a priori x_a. As the same a priori information is used in both, the NDACC and TCCON retrievals, the common a priori is simply the TCCON a priori. The single elements are summed over the profile's pressure levels j, with Δp_j being the pressure difference between two levels. The NIR averaging kernels are mostly solar zenith angle dependent and the Lamont averaging kernels interpolated to the respective zenith angles were used (as suggested by the TCCON database guidelines).

Furthermore, this approach necessitates the knowledge of a true atmospheric profile of the target species (x). As there are no independent measurements of the true atmospheric CO_2 profile with sufficient spatial and temporal coverage available, we use a model profile for this estimation.

As a *true* profile we chose a simulation from NOAA's Carbon Tracker (CT2013) project (CarbonTracker; Peters et al., 2007), linearly interpolated to the site location and to the atmospheric pressure levels used in our retrieval. This allows for an estima-

AMTD
8, 10523–10548, 2015

tion of the influence of the averaging kernel smoothing contribution between the two retrievals.

In Fig. 8, the averaging kernel correction for the Ny-Ålesund time series has been calculated (as shown above) for all data points. Afterwards the data from the different microwindows around 2600 cm^{-1} have been combined and daily averages computed.

The residual in Fig. 8 shows a varying influence of the correction that is associated with the solar zenith angle of the measurements. The magnitude of the correction is solar zenith angle dependent and generally between 1 and −1ppm. Results from the other microwindow regions show comparable behavior.

5 Conclusions

The presented approach for the retrieval of xCO_2 from NDACC MIR microwindows can be used to retrieve information about the total column mole fraction of CO_2. However, further analysis shows a strong sensitivity to the chosen a priori.

The information content of NDACC mid-infrared spectra can constrain the retrieval to robustly reproduce a secular increase of xCO_2. We show, that the tropospheric signal (e.g. the seasonal cycle amplitude) is damped in comparison to TCCON. This can be traced back to the shape of the mid-infrared averaging kernels of the NDACC retrieval, which show little sensitivity in the troposphere and high sensitivity in the stratosphere. The NDACC xCO_2 product can be used for the secular increase, but this does not provide additional information above what is already provided by in situ measurements. The inability to better resolve the seasonal cycle also limits the use of this product for satellite validation. Consequently, we conclude, that these retrievals offer limited value for use in carbon cycle studies.

The greatly different averaging kernels of the two retrievals additionally necessitate the application of a smoothing correction. The magnitude of the averaging kernel smoothing correction has been estimated. It shows a strong dependence on the solar

AMTD
8, 10523–10548, 2015

zenith angle, which originates in the difference in zenith angle dependency of the MIR and NIR averaging kernels. The results show a non-negligible smoothing effect.

A direct comparison of the TCCON and NDACC products remains challenging, due to their complementary sensitivities. Furthermore, the specific sensitivity of the NDACC averaging kernels suggests the possibility of investigating stratospheric changes. We anticipate a full CO_2 profile retrieval (rather than the profile scaling approach used here) will be required to make best use of NDACC mid-infrared spectra in carbon cycle research.

Acknowledgements. The authors would like to thank the station personnel of the AWIPEV station, who operated the instrument. For the estimate of the averaging kernel smoothing error we thankfully acknowledge the NOAA's CarbonTracker program. Funding for this analysis was provided within the ESA Green House Gas Climate Change Initiative (ESA GHG CCI). The operation of the Ny-Ålesund instrument is funded by the EU projects IMECC and GEOmon, and by the Senate of Bremen. Matthias Buschmann received funding from the Earth System Science Research School (ESSReS) and from the German Research Foundation (DFG). Nicholas Deutscher is funded by an Australian Research Council-Discovery Early Career Researcher Award, DE140100178. Additionally we would like to acknowledge the contribution of Frank Hase, Matthias Schneider and Susanne Dohe (KIT, DE) as well as Dan Smale (NIWA, NZ) in the preparation of the final version of this work.

The article processing charges for this open-access publication were covered by the University of Bremen.

References

Barthlott, S., Schneider, M., Hase, F., Wiegele, A., Christner, E., González, Y., Blumenstock, T., Dohe, S., García, O. E., Sepúlveda, E., Strong, K., Mendonca, J., Weaver, D., Palm, M., Deutscher, N. M., Warneke, T., Notholt, J., Lejeune, B., Mahieu, E., Jones, N., Griffith, D. W. T., Velazco, V. A., Smale, D., Robinson, J., Kivi, R., Heikkinen, P., and Raffalski, U.: Using XCO_2 retrievals for assessing the long-term consistency of NDACC/FTIR data sets, Atmos. Meas. Tech., 8, 1555–1573, doi:10.5194/amt-8-1555-2015, 2015. 10525

AMTD
8, 10523–10548, 2015

Buchwitz, M., Reuter, M., Schneising, O., Boesch, H., Guerlet, S., Dils, B., Aben, I., Armante, R., Bergamaschi, P., Blumenstock, T., Bovensmann, H., Brunner, D., Buchmann, B., Burrows, J., Butz, A., Chédin, A., Chevallier, F., Crevoisier, C., Deutscher, N., Frankenberg, C., Hase, F., Hasekamp, O., Heymann, J., Kaminski, T., Laeng, A., Lichtenberg, G., Mazière, M. D., Noël, S., Notholt, J., Orphal, J., Popp, C., Parker, R., Scholze, M., Sussmann, R., Stiller, G., Warneke, T., Zehner, C., Bril, A., Crisp, D., Griffith, D., Kuze, A., O'Dell, C., Oshchepkov, S., Sherlock, V., Suto, H., Wennberg, P., Wunch, D., Yokota, T., and Yoshida, Y.: The Greenhouse Gas Climate Change Initiative (GHG-CCI): comparison and quality assessment of near-surface-sensitive satellite-derived CO_2 and CH_4 global data sets, Remote Sens. Environ., 162, 344–362, doi:10.1016/j.rse.2013.04.024, 2013. 10525

CarbonTracker: CT2013 results provided by NOAA ESRL, NOAA, Boulder, Colorado, USA, available at: http://carbontracker.noaa.gov, last access: 19 May 2014. 10532

Ciais, P., Sabine, C., Bala, G., Bopp, L., Brovkin, V., Canadell, J., Chhabra, A., DeFries, R., Galloway, J., Heimann, M., Jones, C., Le Quéré, C., Myneni, R. B., Piao, S., and Thornton, P.: Carbon and other biogeochemical cycles, Chapter, in: Climate Change 2013: The Physical Science Basis. Contribution of Working Group I to the Fifth Assessment Report of the Intergovernmental Panel on Climate Change, Cambridge University Press, Cambridge, UK and New York, NY, USA, 465–570, 2013. 10524

Goldman, A., Tipping, R., Ma, Q., Boone, C., Bernath, P., Demoulin, P., Hase, F., Schneider, M., Hannigan, J., Coffey, M., and Rinsland, C.: On the line parameters for the (1–0) infrared quadrupolar transitions of $^{14}N_2$, J. Quant. Spectrosc. Ra., 103, 168–174, doi:10.1016/j.jqsrt.2006.05.010, 2007. 10528

Notholt, J., von der Gathen, P., and Peil, S.: Heterogeneous conversion of HCl and $ClONO_2$ during the Arctic winter 1992/1993 initiating ozone depletion, J. Geophys. Res.-Atmos., 100, 11269–11274, doi:10.1029/95JD00850, 1995. 10525

Peters, W., Jacobson, A. R., Sweeney, C., Andrews, A. E., Conway, T. J., Masarie, K., Miller, J. B., Bruhwiler, L. M. P., Pétron, G., Hirsch, A. I., Worthy, D. E. J., van der Werf, G. R., Randerson, J. T., Wennberg, P. O., Krol, M. C., and Tans, P. P.: An atmospheric perspective on North American carbon dioxide exchange: CarbonTracker, P. Natl. Acad. Sci. USA, 104, 18925–18930, doi:10.1073/pnas.0708986104, 2007. 10532

Rodgers, C. D.: Inverse Methods for Atmospheric Sounding: Theory and Practice, Vol. 2, World Scientific, Singapore, 2000. 10529

AMTD
8, 10523–10548, 2015

Rodgers, C. D. and Connor, B. J.: Intercomparison of remote sounding instruments, J. Geophys. Res.-Atmos., 108, 4116, doi:10.1029/2002JD002299, 2003. 10529, 10532

Rothman, L. S., Jacquemart, D., Barbe, A., Chris Benner, D., Birk, M., Brown, L., Carleer, M., Chackerian Jr, C., Chance, K., Coudert, L. E. A., Coudert, L. H., Dana, V., Devi, V. M., Flaud, J.-M., Gamache, R. R., Goldman, A., Hartmann, J.-M., Jucks, K. W., Maki, A. G., Mandin, J.-Y., Massie, S. T., Orphal, J., Perrin, A., Rinsland, C. P., Smith, M. A. H., Tennyson, J., Tolchenov, R. N., Toth, R. A., Vander Auwera, J., Varanasi, P., and Wagner, G.: The HITRAN 2004 molecular spectroscopic database, J. Quant. Spectrosc. Ra., 96, 139–204, 2005. 10527, 10538

Rothman, L. S., Gordon, I. E., Barbe, A., Benner, D. C., Bernath, P. F., Birk, M., Boudon, V., Brown, L. R., Campargue, A., Champion, J.-P., Chance, K., Coudert, L. H., Dana, V., Devi, V. M., Fally, S., Flaud, J.-M., Gamache, R. R., Goldman, A., Jacquemart, D., Kleiner, I., Lacome, N., Lafferty, W. J., Mandin, J.-Y., Massie, S. T., Mikhailenko, S. N., Miller, C. E., Moazzen-Ahmadi, N., Naumenko, O. V., Nikitin, A. V., Orphal, J., Perevalov, V. I., Perrin, A., Predoi-Cross, A., Rinsland, C. P., Rotger, M., Šimecková, M., Smith, M. A. H., Sung, K., Tashkun, S. A., Tennyson, J., Toth, R. A., Vandaele, A. C., and Vander Auwera, J.: The HITRAN 2008 molecular spectroscopic database, J. Quant. Spectrosc. Ra., 110, 533–572, 2009. 10527, 10538

Sussmann, R., Ostler, A., Forster, F., Rettinger, M., Deutscher, N. M., Griffith, D. W. T., Hannigan, J. W., Jones, N., and Patra, P. K.: First intercalibration of column-averaged methane from the Total Carbon Column Observing Network and the Network for the Detection of Atmospheric Composition Change, Atmos. Meas. Tech., 6, 397–418, doi:10.5194/amt-6-397-2013, 2013. 10525

TCCON: TCCON Data Description GGG2012, available at: https://tccon-wiki.caltech.edu/Network_Policy/Data_Use_Policy/Data_Description_GGG2012, (last access: 8 October 2015), 2012. 10532

Wunch, D., Toon, G. C., Blavier, J.-F. L., Washenfelder, R. A., Notholt, J., Connor, B. J., Griffith, D. W. T., Sherlock, V., and Wennberg, P. O.: The Total Carbon Column Observing Network, Philos. T. R. Soc. A, 369, 2087–2112, doi:10.1098/rsta.2010.0240, 2011a. 10525, 10527

Wunch, D., Wennberg, P. O., Toon, G. C., Connor, B. J., Fisher, B., Osterman, G. B., Frankenberg, C., Mandrake, L., O'Dell, C., Ahonen, P., Biraud, S. C., Castano, R., Cressie, N., Crisp, D., Deutscher, N. M., Eldering, A., Fisher, M. L., Griffith, D. W. T., Gunson, M., Heikki-

AMTD
8, 10523–10548, 2015

nen, P., Keppel-Aleks, G., Kyrö, E., Lindenmaier, R., Macatangay, R., Mendonca, J., Messerschmidt, J., Miller, C. E., Morino, I., Notholt, J., Oyafuso, F. A., Rettinger, M., Robinson, J., Roehl, C. M., Salawitch, R. J., Sherlock, V., Strong, K., Sussmann, R., Tanaka, T., Thompson, D. R., Uchino, O., Warneke, T., and Wofsy, S. C.: A method for evaluating bias in global measurements of CO_2 total columns from space, Atmos. Chem. Phys., 11, 12317–12337, doi:10.5194/acp-11-12317-2011, 2011b. 10528, 10532

Yang, Z., Toon, G. C., Margolis, J. S., and Wennberg, P. O.: Atmospheric CO_2 retrieved from ground-based near IR solar spectra, Geophys. Res. Lett., 29, 53-1–53-4, doi:10.1029/2001GL014537, 2002. 10525

AMTD
8, 10523–10548, 2015

Table 1. The mid-IR microwindows used in this study. Each window is characterized by the center wavenumber and its width. Additionally, the corresponding molecular transition is given. Data taken from (Rothman et al., 2005, 2009). Example spectral microwindows are shown in Fig. 1.

Molecule	Center [cm^{-1}]	Width [cm^{-1}]	Quantum transition	Line intensity [cm^{-1} (molecule cm^{-2})]	Lower state energy [cm^{-1}]
$^{16}O^{12}C^{18}O$	2620.83	0.55	20002 → 00001	3.270×10^{-25}	26.5087
$^{16}O^{12}C^{18}O$	2626.63	0.45	20002 → 00001	4.309×10^{-25}	100.1374
$^{16}O^{12}C^{18}O$	2627.35	0.50	20002 → 00001	4.291×10^{-25}	112.6533
$^{16}O^{12}C^{18}O$	2629.61	0.67	20002 → 00001	4.076×10^{-25}	154.6166
$^{16}O^{12}C^{16}O$	3160.22	0.16	21103 → 00001	3.140×10^{-25}	316.7698
$^{16}O^{12}C^{16}O$	3161.70	0.20	21103 → 00001	3.030×10^{-25}	273.868
$^{16}O^{12}C^{16}O$	3315.78	0.55	21102 → 00001	1.726×10^{-24}	362.7882
$^{16}O^{12}C^{16}O$	3344.81	0.26	21102 → 00001	7.747×10^{-25}	16.389

AMTD
8, 10523–10548, 2015

Table 2. Overview over the estimated errors from the different retrievals. Given are both the mean standard deviation of the daily mean and the mean standard error for N measurements, in ppm.

	TCCON	2600 cm^{-1}	3100 cm^{-1}	3300 cm^{-1}
σ	1.13	2.06	3.21	1.16
$\sigma/\sqrt{N}$	0.23	0.96	1.67	0.60

AMTD
8, 10523–10548, 2015

Table 3. Fit parameters corresponding to the fits of the time series in Fig. 6 and in Eq. (3). Units are xCO_2 in ppm as a function of time in decimal years starting 1 January 2009. Uncertainty estimates are 1σ fitting errors.

retrieval	a [ppm]	b [ppm yr^{-1}]	A [ppm]
TCCON	383.27 ± 0.20	2.23 ± 0.09	5.73 ± 0.14
TCCON fixed	383.55 ± 0.19	2.21 ± 0.08	6.55 ± 0.14
NDACC	381.93 ± 0.64	2.41 ± 0.24	5.60 ± 0.49
NDACC fixed	381.08 ± 0.67	2.44 ± 0.28	2.64 ± 0.50

AMTD
8, 10523–10548, 2015

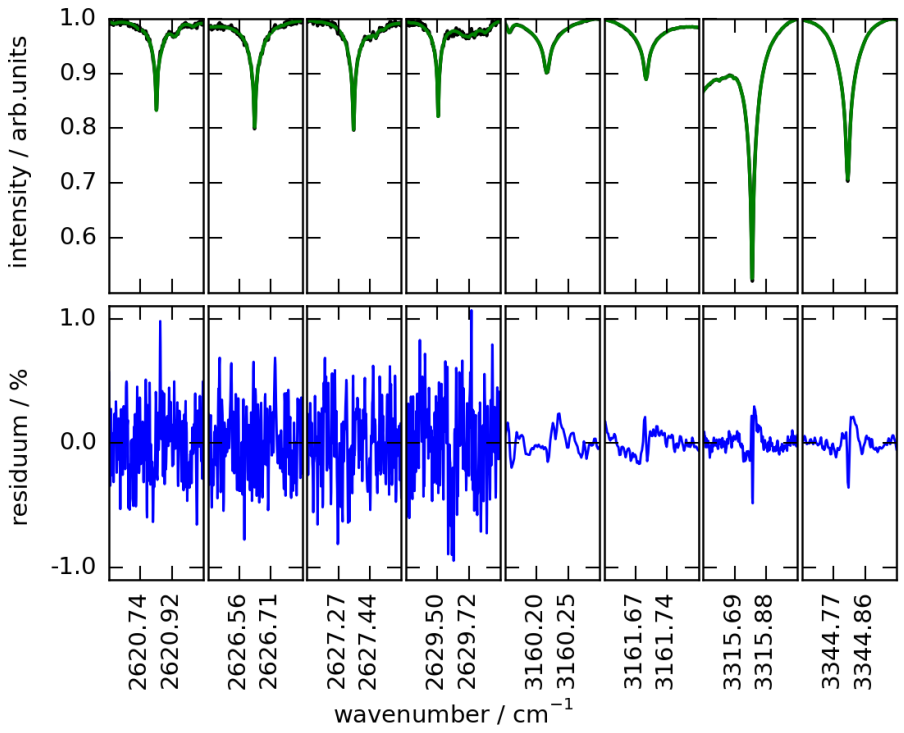

Figure 1. An example fit of the measured (black) with the calculated (green) spectrum and their residuals (blue) for the various micro windows used. Note the different signal-to-noise ratio due to different instrument setup (see Sect. 2.2).

AMTD
8, 10523–10548, 2015

MIR xCO_2 retrieval and comparison to TCCON

M. Buschmann et al.

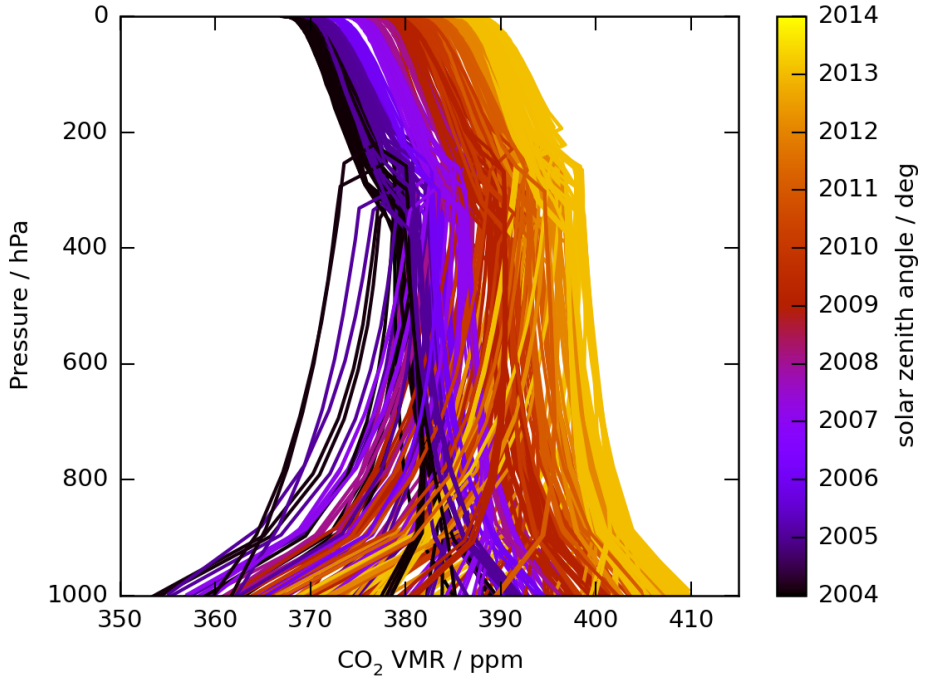

Figure 2. The TCCON a priori profiles calculated for Ny-Ålesund and the time frame of this analysis.

AMTD
8, 10523–10548, 2015

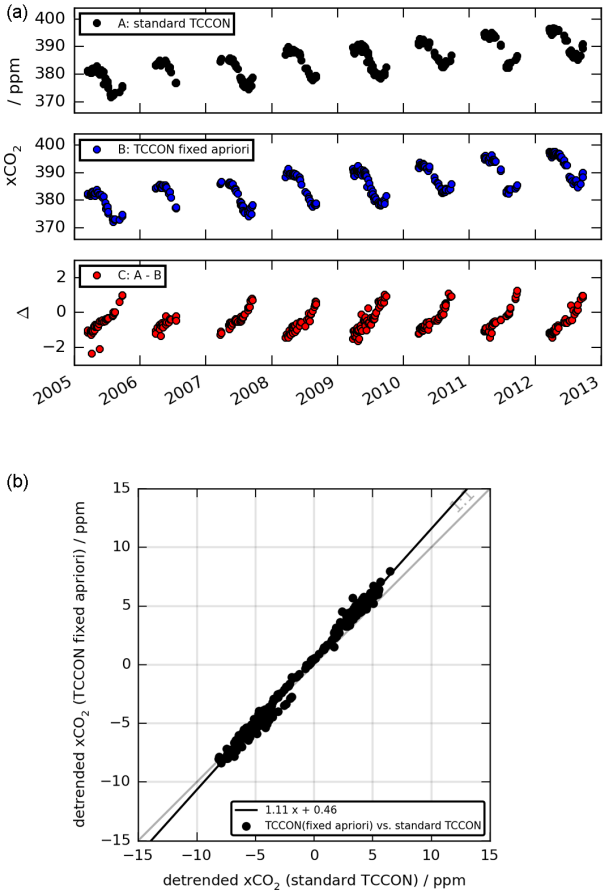

Figure 3. (a) xCO_2 from the TCCON standard window for retrievals using the TCCON (upper panel) and fixed (center panel) a priori and their difference (lower panel). **(b)** The corresponding correlation plot of the detrended xCO_2 time series of the TCCON standard window, with modeled and fixed a priori.

AMTD
8, 10523–10548, 2015

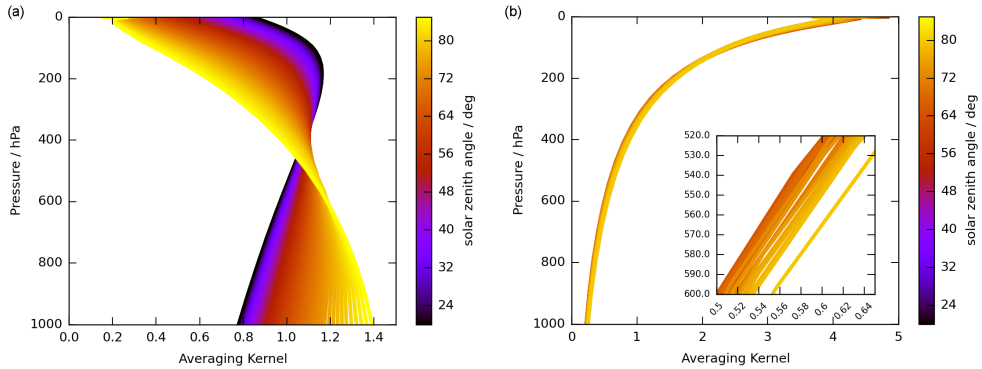

Figure 4. Left: the total column averaging kernels from the TCCON retrievals. The official averaging kernels from the Lamont site, linearly interpolated to obtain intermediate profiles. Note the minimal possible solar zenith angle in Ny-Ålesund is 55°. Right: the total column averaging kernels from the 2626 cm^{-1} microwindow as an example NDACC averaging kernel. Note the high sensitivity in the stratosphere and low sensitivity in the troposphere in comparison to TCCON.

AMTD
8, 10523–10548, 2015

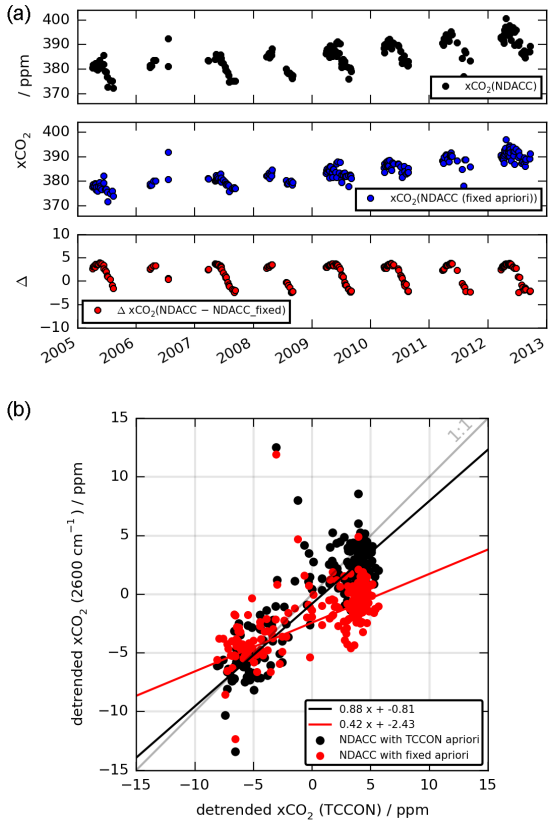

Figure 5. (a) xCO_2 from the 2600 cm^{-1} NDACC spectra for retrievals using a modelled (upper panel) and fixed (center panel) a priori and their differences (lower panel). No residual secular trend is evident in the residuum. A clear seasonal pattern is visible, thus a big part of the seasonal cycle is damped, when using a fixed a priori. **(b)** The corresponding correlation plot of the de-trended xCO_2 time series of TCCON vs. the NDACC retrievals with modeled and fixed a priori.

AMTD
8, 10523–10548, 2015

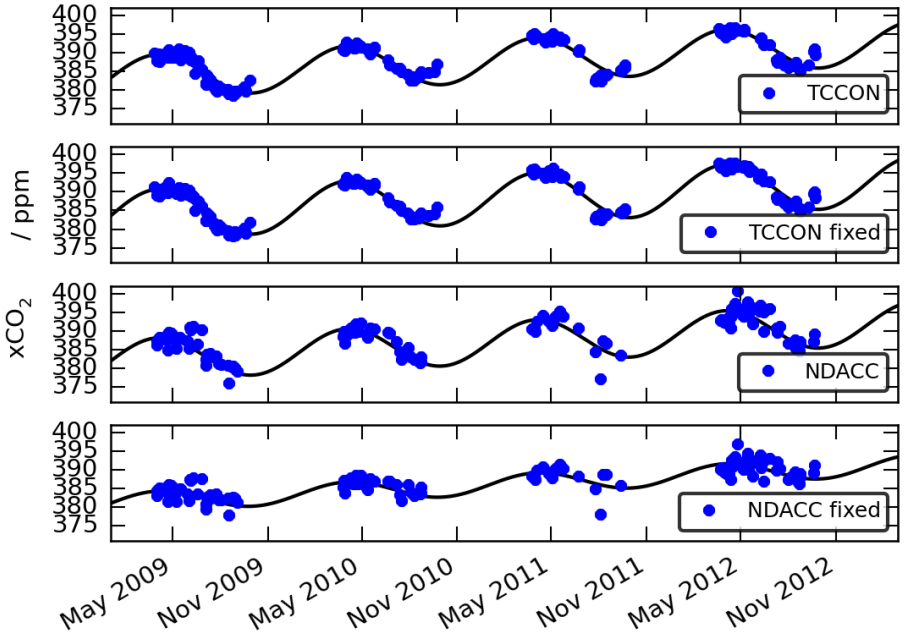

Figure 6. Fits to the different retrievals. Top two panels: standard TCCON retrieval and TCCON retrieval with fixed a priori. Bottom two panels: NDACC with TCCON and fixed a priori respectively. The fit parameters corresponding to Eq. (3) are presented in Table 3. For clarity, only a subset of the data from 2009 to 2013 is shown.

AMTD
8, 10523–10548, 2015

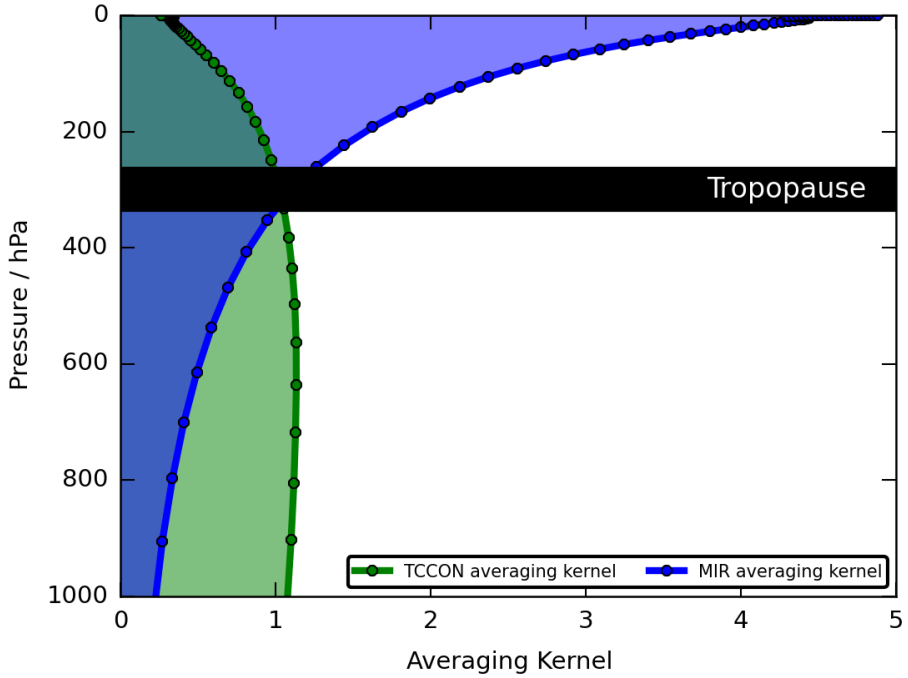

Figure 7. Visualization of the tropospheric and stratospheric contribution of the MIR (blue) and TCCON (green) averaging kernels for an example solar zenith angle of 69°.

AMTD
8, 10523–10548, 2015

MIR xCO_2 retrieval and comparison to TCCON

M. Buschmann et al.

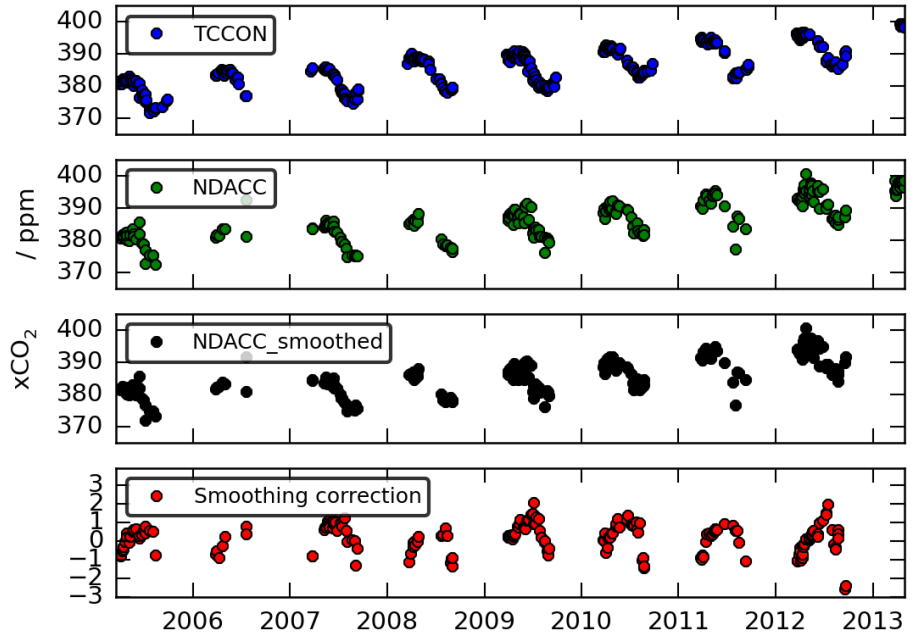

Figure 8. An estimate of the magnitude of the averaging kernel smoothing correction as described in Eq. (4) for the Ny-Ålesund time series of the 2600 cm^{-1} windows with CarbonTracker2013 as a *true* atmospheric profile.

AMTD
8, 10523–10548, 2015